Biointerface Research in Applied Chemistry
Open-Access Journal (ISSN: 2069-5837)

Article
Volume 13, Issue 2, 2023, 175
https://doi.org/10.33263/BRIAC132.175

Photoluminescence Studies on $LiNa_5(PO_4)_2:Eu^{3+}$ Phosphor

Miyapuram Ravi [1], Ghanta Pushpa Chakrapani [2], Bezawada Mahitha [2], Karnati Srinivasulu [2], Porala Jayanth kumar [2], Gurram Giridhar [2,*]

[1] Department of Physics, Dr. B.R. Ambedkar Open University, Telangana, India
[2] Department of Nanotechnology, Acharya Nagarjuna University, A.P., India
* Correspondence: drggiridhar@rediffmail.com (G.G.);

Scopus Author ID 23972881700
Received: 12.02.2022; Accepted: 13.03.2022; Published: 30.03.2022

Abstract: In this paper, $LiNa_5(PO_4)_2:Eu^{3+}$, a new class of phosphor, was prepared with different concentrations of Eu^{3+} by solution combustion synthesis. This series of prepared materials were investigated by using various experimental techniques. X-ray diffraction confirmed a consistent orthorhombic phase and agreed with the standard JCPDF data. This phosphor exhibits intense d red emission peaks at ~612 nm corresponding to $^5D_0$–$^7F_2$ transition upon 392 nm excitation. The color of the emitting light is red, and the calculated chromaticity coordinates are well placed in the red region. The results indicate that the present phosphors could be the potential candidates for the source of red color both in lasers and in light-emitting diodes.

Keywords: phosphor; X-ray diffraction; emission; excitation; red emission.

1. Introduction

Nowadays, phosphors have great interest in the development of display and lighting devices. Various hosts like borates, aluminates, silicates, etc., are well known for commercial phosphors due to their chemical and thermal stability [1]. Among these hosts, phosphates are considered good because of their high acceptance of dopants, low synthesis temperatures, and chemical and thermal durability. So these materials are appearing continuously as potential candidates for luminescence applications. This kind of material is not only for optical applications but also useful for nonlinear optical applications with structure-property relationships [2]. Moreover, among various rare-earths ions, Eu^{3+} is an important source of red light due to its simple energy level structure, which explains the local environment of these ions with its characteristic transition intensities [3–5].

In search of high-performance phosphors for different multifunctional applications [6], Eu^{3+} doped phosphate phosphors had their significance [7,8] to support a pure white light generation [9–14]. In this context, we are working with this $LiNa_5(PO_4)_2$ host with different rare-earth ions [15]. However, no work has been reported earlier on Eu^{3+} ions doped $LiNa_5(PO_4)_2$. Therefore, this study investigated the luminescence properties with varied dopant concentrations by excitation and emission spectra with decay profiles.

2. Materials and Methods

$LiNa_{5-x}(PO_4)_2:xEu^{3+}$ where x = 0, 0.1, 0.3 and 0.5 mol%; phosphors were prepared by using solution combustion method. $LiNO_3$, $NaNO_3$, Eu_2O_3, and $(NH_4)H_2PO_4$ are used to

prepare the samples. All precursors were taken in stoichiometric ratio and urea and mixed in a mortar to obtain a uniform mix. Oxide materials were converted to Nitrates by dissolving in Nitric acid. Further, Boric acid is used as a flux. The precursors' concentration was calculated by following the procedure reported by K.N. Shinde *et al*. [16]. Each batch (20 g) with a different concentration of Eu^{3+} was mixed well in an agate mortar and kept in a high-temperature furnace at 800 ^{o}C. In a few minutes (3-4 minutes), the reaction occurred, and solid white foam remained in the crucible. The resultant sample was ground and annealed at 650 ^{o}C for 3h for thermal stabilization. All the characterization of samples was done at room temperature. X-ray diffraction patterns were obtained from SHIMADZU LabX DRD-6100 diffractometer with Cu-Kα radiation. Photoluminescence–emission and excitation spectra were measured with a Thermo spectrophotometer. Decay profiles were measured by using Edinburgh Instruments FLSP 920 system.

3. Results and Discussion

X-ray diffraction patterns of prepared (a) $LiNa_5(PO_4)_2$ (pure), (b) $LiNa_5(PO_4)_2$:0.1Eu^{3+} and (c) $LiNa_5(PO_4)_2$:0.3Eu^{3+}, (d) $LiNa_5(PO_4)_2$:0.5Eu^{3+} were shown in Fig 1 and are confirmed the well-crystallized orthorhombic structure(JCPDS No.77-0996) in all the samples. Further, no such considerable changes were observed with the addition of dopant. We also used the Reitveld refinement method to determine the crystal structure of the prepared $LiNa_5(PO_4)_2$:0.5Eu^{3+} sample.

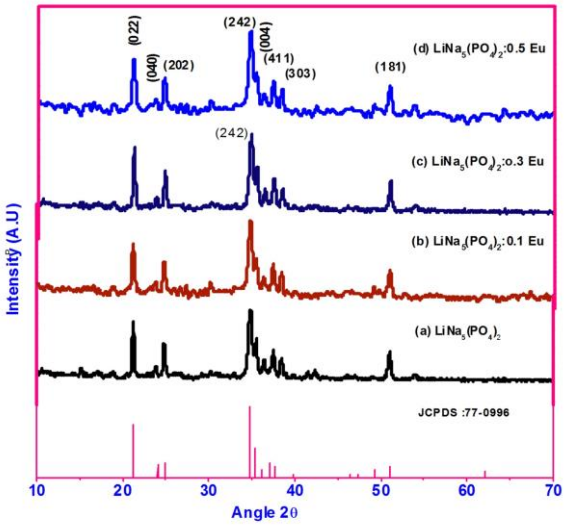

Figure 1. X-ray diffraction patterns of Eu3+ doped $LiNa_5(PO_4)_2$ phosphors

The standard structure (JCPDS No.77-0996) was taken to initiate the procedure, and the obtained result is shown in Figure 2. The result shows that the prepared sample is in an orthorhombic structure with the space group of $P2_12_12_1$, and the lattice parameters are a = 10.095 Å, b = 14.842 Å, c = 10.163 Å, V = 1522..87 $Å^3$, and the refinement parameters are R_p =7.69, R_{wp} =8.16, $\chi 2$ = 1.79; which indicates the good match of standard structure (V = 1517.51 Å) and resembles the isostructure of $LiNa_5(PO_4)_2$. The slight variation in the cell volume is due to the radius of Eu^{3+}. No impure phases were found and demonstrated the occupation of Eu^{3+} (r = 0.95 Å) to Na^{+} (1.02 Å) sites in the host [6]. Visualization for Electronic and Structure Analysis (VESTA) program [17] is utilized to generate the crystal structure of the unit cells with the obtained lattice parameters (Figure.3).

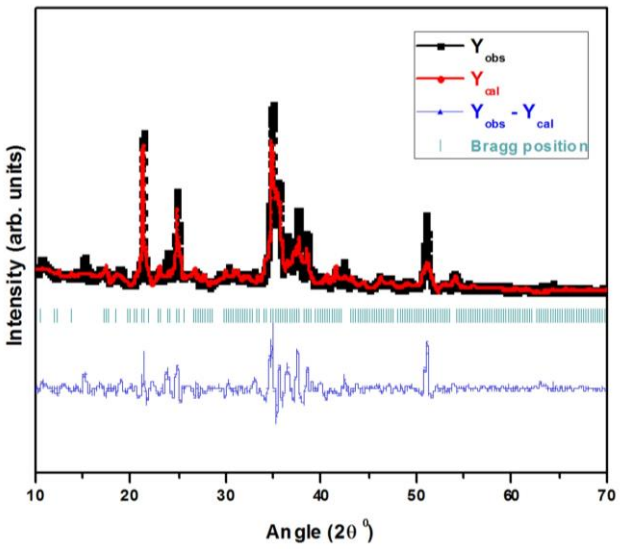

Figure 2. Reitveld refinement of $LiNa_5(PO_4)_2$: 0.5 Eu^{3+}.

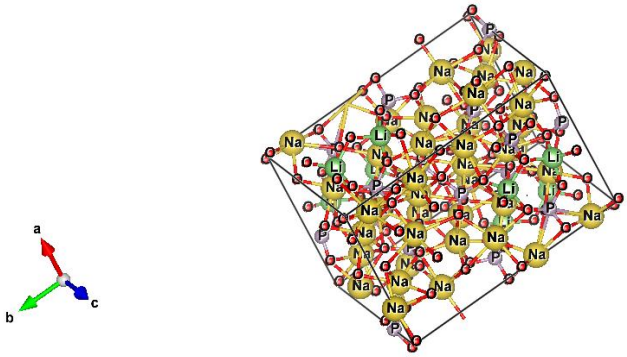

Figure 3. Unit cell of $LiNa_5(PO_4)_2$.

The excitation spectra were recorded by monitoring 612 nm wavelength. Similar spectrums were observed for all the samples, and Eu^{3+} spectrum [18,19] is shown in Figure 4 for clear visibility of excitation peaks. The excitation bands observed at 360 nm, 392 nm, 413 nm, 463 nm, and 531 nm are assigned to intra $4f^6$ absorption transitions of Eu^{3+} from $^7F_0$ to $^6D_4$, $^6L_7$, $^6L_8$, $^6D_3$, and $^6D_0$, respectively. The transition $^7F_0 \rightarrow {}^6L_7$ at 392 nm is with maximum intensity, which means that $^6L_7$ level is acting as a metastable state and consists of a maximum number of absorbed photons [20].

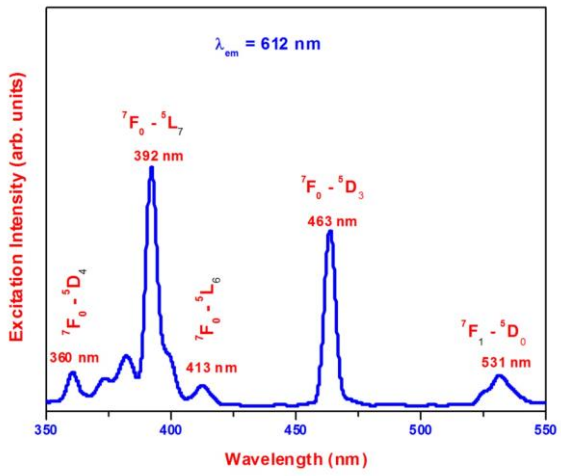

Figure 4. The excitation spectrum of $LiNa_5(PO_4)_2$:0.5 Eu^{3+} phosphor.

The optical excitation is done by the light (392 nm) from the xenon lamp through a monochromator and measured by the emission spectra for the present phosphors shown in Figure 5. The photoluminescence emission spectra consist of a series of well-resolved emission bands at 589 nm, 611 nm, 651 nm, and 701 nm, which can be assigned to the emission transition $^5D_0 \rightarrow {}^7F_1$, $^5D_0 \rightarrow {}^7F_2$, $^5D_0 \rightarrow {}^7F_3$ and $^5D_0 \rightarrow {}^7F_4$. It shows the splitting of the Eu^{3+} 4f shall as $^5D_0 - {}^7F_J$ (J = 1, 2, 3 and 4)[1,10,18] for all the phosphor powders.

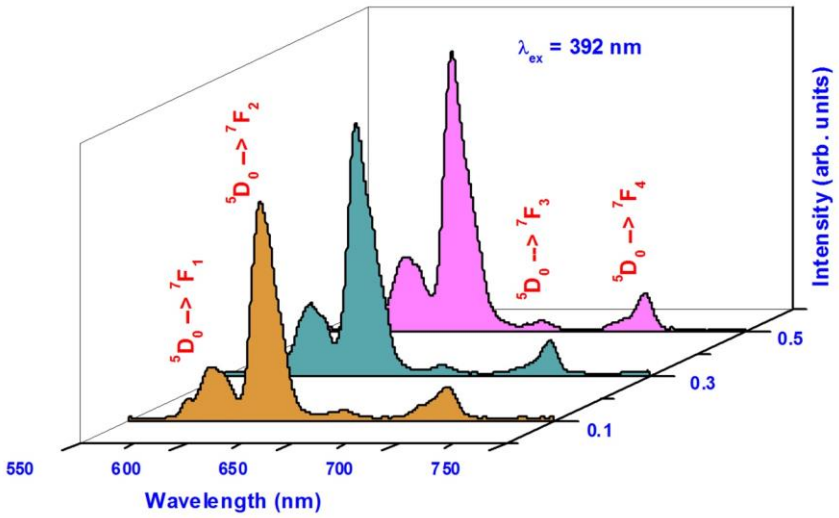

Figure 5. Emission spectra of $LiNa_5(PO_4)_2$: Eu^{3+} phosphors.

Here we can see a gradual increase in the intensity of the emission peaks with the concentration of Eu^{3+}, showing the dependence of emission intensity on the concentration of dopant [3,4,13]. It is a well-known fact that a magnetic dipole transition depends on crystal field strength and electric dipole transition on the local electric field around Eu^{3+} ions. In addition, the allowed electric dipole transition is hypersensitive to the local symmetry around the rare earth ion. In the case of these Eu^{3+} doped $LiNa_5(PO_4)_2$ phosphors, the $^5D_0 \rightarrow {}^7F_1$(589 nm) is magnetic dipole transition, and the $^5D_0 \rightarrow {}^7F_2$(611 nm) is electric dipole as well. The high intensity of $^5D_0 \rightarrow {}^7F_2$ also demonstrates the increasing distortion of the local field around the Eu^{3+} ions [7,21–24], i.e., Eu^{3+} ions process no inversion symmetry at sites.

Further, one can measure the degree of distortion from the inversion symmetry of the local environment of Eu^{3+} ions by calculating the asymmetric ratio, the intensity ratio between $^5D_0 \rightarrow {}^7F_1$ and $^5D_0 \rightarrow {}^7F_2$. Figure 5 shows that the asymmetry ratio increases with dopant concentration and suggests the symmetry distortion of the local environment around Eu^{3+} ions in the present host due to different sizes of Na^+ and Eu^{3+}. On the other side, charge compensation is needed to replace Eu^{3+} in Na^+ sites, which raises the defects in the host and lowers the symmetry of the local environment as a consequence [25]. These results significantly show the existence of nonradiative recombination centers and are helpful to the host to be a potential candidate for nonlinear optical applications.

Figure 6 shows the decay profiles of $LiNa_5(PO_4)_2$: Eu^{3+} phosphors. The decay profiles were fitted with a single exponential function, $I = I_0 e^{-t/\tau}$, where τ is the decay lifetime. The estimated lifetimes are 1.9 ms, 2.17ms, and 2.5 ms for 0.1, 0.3, and 0.5 mol% of $Eu^{3+,}$ respectively. These values were increased with increasing Eu3+ concentration, which also supports the increase in the number of luminescent centers without crystal field effects [5,23,26–28].

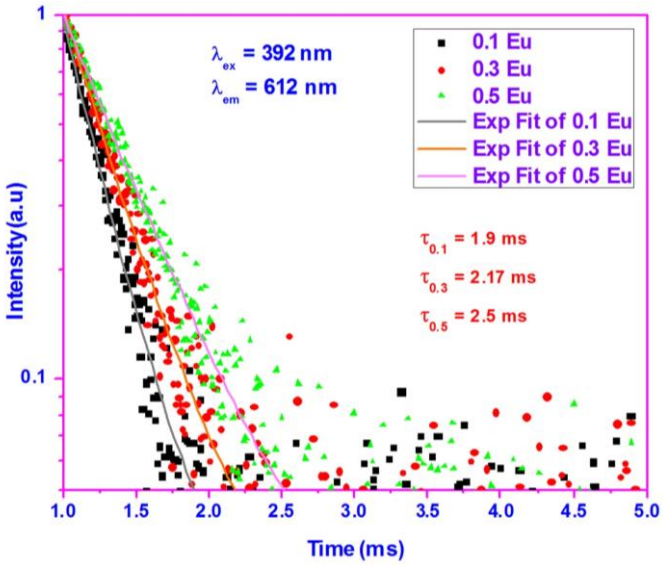

Figure 6. Decay profiles of $LiNa_5(PO_4)_2$: Eu^{3+} phosphors

Commission Internationale de l'Eclairage (CIE) coordinates were estimated for $LiNa_5(PO_4)_2$: Eu^{3+} phosphors, which are frequently used to examine and express colors of phosphors[29,30] and are shown in Figure 7. The color purity and CCT values were also estimated by using color calculator v7.77 and other formulae. The estimated values are given in Table 1.

Table 1. CIE color coordinates with CCT values.

Sample	CIE Coordinates (x,y)	CCT (K)	Colour Purity
$LiNa_5(PO_4)_2$: 0.1Eu^{3+}	(0.634, 0.352)	1099	91.04 %
$LiNa_5(PO_4)_2$: 0.3Eu^{3+}	(0.641, 0.342)	1032	92.53 %
$LiNa_5(PO_4)_2$: 0.5Eu^{3+}	(0.647, 0.346)	1027	93.72 %

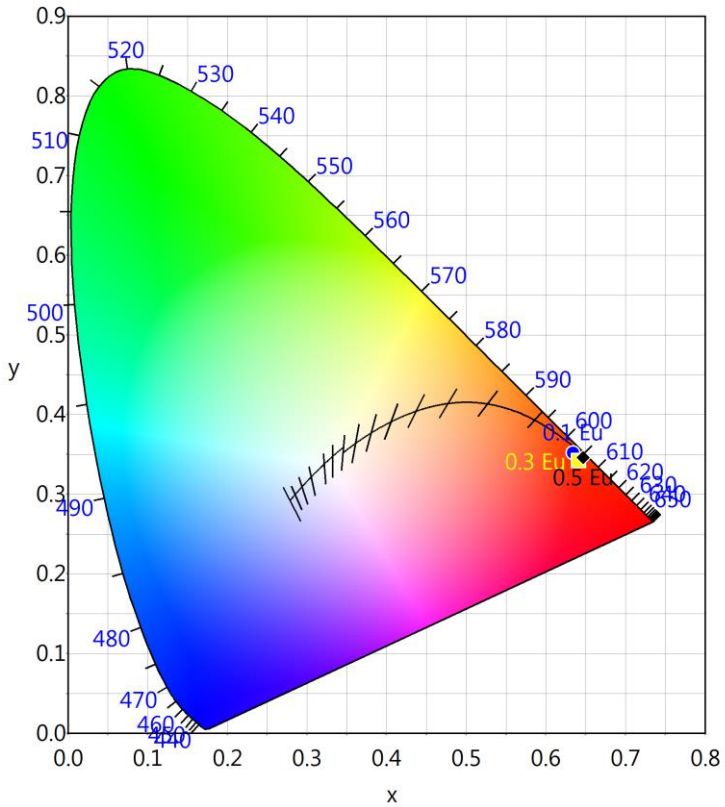

Figure 7. CIE diagram of $LiNa_5(PO_4)_2$:xEu^{3+} (x = 0.1, 0.3 and 0.5 mol%) phosphors.

The coordinates and the corresponding color purity values of the present phosphors indicate that the phosphors are suitable candidates for efficient red emission. So these phosphors are useful for developing both display and light-emitting diodes.

4. Conclusions

$LiNa_5(PO_4)_2$: Eu^{3+} phosphors were prepared using solution combustion synthesis. Eu^{3+} ions were successfully placed in the host without altering the structure, confirmed by Xray diffraction studies with refinement. A small variation occurred in unit cell volume by doping the Eu^{3+} ions. Photoluminescence intensity increased with an increase in Eu^{3+} concentration is related to both no symmetry distortion and enhancement of luminescent centers and consequent nonradiative recombination centers. Decay profiles also support the results shown by the phosphors. CIE coordinates were well placed in the red region and indicate that these phosphors are promising candidates for red emission.

Funding

This research received no external funding.

Acknowledgments

The authors are thankful to the Department of Physics, KLCE, Vaddeswaram, Guntur, for providing an X-ray diffraction facility.

Conflicts of Interest

The authors declare no conflict of interest.

References

1. Zhao, J.; Dong, J.; Ye, X.; Wang, L. A promising novel red-emitting Eu3+-activated neodymium calcium phosphate phosphor with good thermal stability and excellent color purity for WLEDs. *J. Mol. Struct.* **2021**, *1240*, 130567, https://doi.org/10.1016/j.molstruc.2021.130567.
2. Li, L.; Wang, Y.; Lei, B.-H.; Han, S.; Yang, Z.; Poeppelmeier, K.R.; Pan, S. A New Deep-Ultraviolet Transparent Orthophosphate $LiCs_2PO_4$ with Large Second Harmonic Generation Response. *J. Am. Chem. Soc.* **2016**, *138*, 9101–9104, https://doi.org/10.1021/jacs.6b06053.
3. Munirathnam, K.; Dillip, G.R.; Raju, B.; Joo, S.W.; Dhoble, S.J.; Nagabhushana, B.M.; Hari Krishna, R.; Ramesh, K.P.; Varadharaj Perumal, S.; Prakashbabu, D. Synthesis, photoluminescence and Judd–Ofelt parameters of $LiNa_3P_2O_7$: Eu^{3+} orthorhombic microstructures. *Appl. Phys. A* **2015**, *120*, 1615–1623, https://doi.org/10.1007/s00339-015-9371-1.
4. Yu, B.; Li, Y.; Wang, Y.; Geng, L. Double-site Eu^{3+} occupation in the langbeinite-type phosphate phosphor toward adjustable emission for pc-WLEDs. *J. Alloys Compd.* **2021**, *874*, 159862, https://doi.org/10.1016/j.jallcom.2021.159862.
5. Verma, B.; Baghel, R.N.; Bisen, D.P.; Brahme, N.; Jena, V. Judd-Ofelt analysis and luminescent characterization of Eu^{3+} activated Li_2Zr $(PO_4)_2$ phosphor. *Opt. Mater.* **2021**, *118*, 111196, https://doi.org/10.1016/j.optmat.2021.111196.
6. Wang, C.; Li, Y.; Chen, S.; Li, Y.; Lv, Q.; Shao, B.; Zhu, G.; Zhao, L. A novel high efficiency and ultra-stable red emitting europium doped pyrophosphate phosphor for multifunctional applications. *Inorg. Chem. Front.* **2021**, *8*, 3984–3997, https://doi.org/10.1039/d1qi00528f.
7. Duragkar, A.; Kohale, R.L.; Dhoble, N.S.; Dhoble, S.J. Tunable luminescence of Eu^{3+}, Sm^{3+} and Dy^{3+} doped Na_2CaMg $(PO_4)_2$ phosphor for optical applications. *J. Mol. Struct.* **2020**, *1199*, 126969, https://doi.org/10.1016/j.molstruc.2019.126969.
8. Hingwe, V.S.; Bajaj, N.S.; Omanwar, S.K. Eu^{3+} doped N-UV emitting $LiSrPO_4$ phosphor for W-LED application. *Opt. J. Light Electron Opt.* **2017**, *130*, 149–153, https://doi.org/10.1016/j.ijleo.2016.11.025.
9. Fan, G.; Wang, L.; Hu, R.; Fan, D. A white LED with orange-red phosphors $KBaBP_2O_8$: Eu^{3+}. *Inorg. Chem. Commun.* **2021**, *127*, 108527, https://doi.org/10.1016/j.inoche.2021.108527.

10. Xiong, J.; Li, G.; Li, D.; Pun, E.Y.B.; Lin, H. Color tunability imparted by multi-peak emissions of Eu^{3+} in fluoride-phosphate phosphors. *Mater. Chem. Phys.* **2021**, *274*, 125167, https://doi.org/10.1016/j.matchemphys.2021.125167.
11. Meena, M.L.; Lu, C.-H.; Som, S.; Chaurasiya, R.; Lin, S.D. Highly efficient and thermally stable Eu^{3+} activated phosphate based phosphors for wLEDs: An experimental and DFT study. *J. Alloys Compd.* **2022**, *895*, 162670, https://doi.org/10.1016/j.jallcom.2021.162670.
12. Xiao, Z.; Zhang, Z.; Li, J.; Zhang, B.; Wu, B.; Wang, F.; Liu, W.; Song, J.; Han, L.; You, W. Preparation and luminescent properties of $Y_2Zr_2O_7$: Eu_{3+} phosphor for W-LED application. *Appl. Phys. A* **2021**, *127*, 1–10, https://doi.org/10.1007/s00339-021-05024-4.
13. Wu, X.; Du, L.; Ren, Q.; Zhao, Y.; Hai, O. Synthesis and luminescent properties of $LiLaSiO_4$: Dy^{3+}, Eu^{3+} phosphors for white LEDs. *J. Solid State Chem.* **2021**, *293*, 121798, https://doi.org/10.1016/j.jssc.2020.121798.
14. Yu, P.; Guo, W.; Zhang, R.; Su, L.; Xu, J. White and tunable light emission in Eu3+, Dy3+ codoped phosphate glass. *Opt. Mater. (Amst).* **2021**, *114*, 110939, https://doi.org/10.1016/j.optmat.2021.110939.
15. Ravi, M.; Chakrapani, G.P.; Balachandrika, M.; Vasudevarao, P.; Nageswararao, C.; Babu, L.K.K.; Prasad, P.M.; Giridhar, G. Photoluminescence studies on $LiNa_5$ $(PO_4)_2$: Dy^{3+}, Sm^{3+} phosphor. *Zeitschrift für Naturforsch. A* **2021**, https://doi.org/10.1515/zna-2021-0153.
16. Shinde, K. N., Dhoble, S. J., Swart, H. C., & Park, K. *Introduction. In: Phosphate Phosphors for Solid-State Lighting.*; **2013**; Vol. 174; ISBN 9783642334504, https://doi.org/10.1007/978-3-642-34312-4_8.
17. Momma, K.; Izumi, F. VESTA 3 for three-dimensional visualization of crystal, volumetric and morphology data. *J. Appl. Crystallogr.* **2011**, *44*, 1272–1276, https://doi.org/10.1107/S0021889811038970.
18. Cherbib, M.A.; Khattech, I. Structure and peculiar luminescence of Eu^{3+}-doped sodium/alkaline earths phosphate glasses. *J. Lumin.* **2021**, *239*, 118349, https://doi.org/10.1016/j.jlumin.2021.118349.
19. Chen, Q.; Hao, Y.; Chen, Q. Eu^{2+} activated novel eulytite Na_3Bi_5 $(PO_4)_6$: Eu^{3+} phosphors: Enhanced luminescence and thermal stability for photonics application. *Ceram. Int.* **2022**., https://doi.org/10.1016/j.ceramint.2022.02.046.
20. Zhou, L.; Ye, R.; Liu, F.; Lin, J.; Chen, Y.; Fu, J.; Guo, W.; Deng, D.; Xu, S. Dual-emitting from Bi^{3+}/Eu^{3+} co-activated akermanite phosphor for optical thermometric applications. *Opt. Mater.* **2021**, *116*, 111076, https://doi.org/10.1016/j.optmat.2021.111076.
21. Singh, S. Enhancement and luminescence properties of Eu^{3+}, Sm^{3+} co-doped $KMgPO_4$ phosphor with variable concentration of Eu^{3+} for w-LEDs. *Bull. Mater. Sci.* **2021**, *44*, 1–5, https://doi.org/10.1007/s12034-020-02314-0.
22. Li, Y.-N.; Zhao, D.; Shi, L.-Y.; Dai, S.-J.; Fan, Y.-P.; Liu, B.-Z.; Yao, Q.-X. Enhanced luminescence of a new red phosphor $Na_{13}Sr_2Ta_2$ $(PO_4)_9$: Eu^{3+} by co-doping charge compensators Li^+/Na^+/K^+. *J. Lumin.* **2020**, *220*, 116976, https://doi.org/10.1016/j.jlumin.2019.116976.
23. Meza-Rocha, A.N.; Speghini, A.; Bettinelli, M.; Caldiño, U. Orange and reddish-orange light emitting phosphors: Sm^{3+} and Sm^{3+}/Eu^{3+} doped zinc phosphate glasses. *J. Lumin.* **2015**, *167*, 305–309, https://doi.org/10.1016/j.jlumin.2015.06.050.
24. Wang, Z.Y.; Shen, B.L.; Yu, K.H.; Yang, Z.; Zheng, R.L.; Hu, E.T.; Zheng, J.J.; Wei, W. Tunable white-light emission of Dy^{3+} or/and Eu^{3+} co-doped single-phase $LiY(PO_3)_4$ phosphors for NUV-WLEDs. *J. Alloys Compd.* **2019**, *791*, 833–838, https://doi.org/10.1016/j.jallcom.2019.03.406.
25. Dai, S.; Zhang, W.; Zhou, D.; Yan, G.; Liu, S. Effect of A^+ (A = Li, Na and K) co-doping on the luminescence enhancement of $CaSr_2(PO_4)_2$:Dy^{3+} phosphors for white light-emitting diodes. *Ceram. Int.* **2017**, *43*, 15493–15499, https://doi.org/10.1016/j.ceramint.2017.08.097.
26. Langar, A.; Bouzidi, C.; Elhouichet, H.; Gelloz, B.; Ferid, M. Investigation of spectroscopic properties of Sm-Eu codoped phosphate glasses. *Displays* **2017**, *48*, 61–67, https://doi.org/10.1016/j.displa.2017.03.004.
27. Yu, M.; Zhang, W.; Yan, G.; Dai, S.; Qiu, Z.; Zhang, L. Warm white emission property of Ca_2Sr $(PO_4)_2$: Dy^{3+} phosphors with red compensation by Eu^{3+} co-doping. *Ceram. Int.* **2018**, *44*, 2563–2567, https://doi.org/10.1016/j.ceramint.2017.11.012.
28. Pawlik, N.; Szpikowska-Sroka, B.; Goryczka, T.; Pisarski, W.A. Photoluminescence investigation of sol-gel glass-ceramic materials containing SrF_2: Eu^{3+} nanocrystals. *J. Alloys Compd.* **2019**, *810*, 151935, https://doi.org/10.1016/j.jallcom.2019.151935.
29. Yang, Z.; Li, T.; Li, P.; Wang, Z.; Xu, S.; Bai, Q.; Dong, H. Synthesis and luminescence properties of novel white emitting phosphor $KMgLa(PO_4)_2$:Dy^{3+}. *J. Lumin.* **2016**, *178*, 178–182, https://doi.org/10.1016/j.jlumin.2016.05.053.
30. Chandana, G.; Nageswara Rao, C.; Vasudeva Rao, P.; Al-Musawi, M.J.S.; Samatha, K.; Dhar, G.G. Luminescent properties of Sm^{3+} doped metal fluoro phosphate glasses. *Optik* **2020**, *208*, 163909, https://doi.org/10.1016/j.ijleo.2019.163909.